Geophysical Journal International

Geophys. J. Int. (2015) **200,** 664–675 doi: 10.1093/gji/ggu409

GJI Geomagnetism, rock magnetism and palaeomagnetism

Geodynamo model and error parameter estimation using geomagnetic data assimilation

Andrew Tangborn[1] and Weijia Kuang[2]

[1]*Joint Center for for Earth Sciences Technology, University of Maryland-Baltimore County, Baltimore, MD, USA. E-mail: tangborn@umbc.edu*

[2]*Space Geodesy Laboratory, Code* 697*, Goddard Space Flight Center, Greenbelt, MD, USA*

Accepted 2014 October 16. Received 2014 October 14; in original form 2014 May 13

SUMMARY

We have developed a new geomagnetic data assimilation approach which uses the minimum variance' estimate for the analysis state, and which models both the forecast (or model output) and observation errors using an empirical approach and parameter tuning. This system is used in a series of assimilation experiments using Gauss coefficients (hereafter referred to as observational data) from the GUFM1 and CM4 field models for the years 1590–1990. We show that this assimilation system could be used to improve our knowledge of model parameters, model errors and the dynamical consistency of observation errors, by comparing forecasts of the magnetic field with the observations every 20 yr. Statistics of differences between observation and forecast ($O - F$) are used to determine how forecast accuracy depends on the Rayleigh number, forecast error correlation length scale and an observation error scale factor. Experiments have been carried out which demonstrate that a Rayleigh number of 30 times the critical Rayleigh number produces better geomagnetic forecasts than lower values, with an Ekman number of $E = 1.25 \times 10^{-6}$, which produces a modified magnetic Reynolds number within the parameter domain with an 'Earth like' geodynamo. The optimal forecast error correlation length scale is found to be around 90 per cent of the thickness of the outer core, indicating a significant bias in the forecasts. Geomagnetic forecasts are also found to be highly sensitive to estimates of modelled observation errors: Errors that are too small do not lead to the gradual reduction in forecast error with time that is generally expected in a data assimilation system while observation errors that are too large lead to model divergence. Finally, we show that assimilation of $L \leq 3$ (or large scale) gauss coefficients can help to improve forecasts of the $L > 5$ (smaller scale) coefficients, and that these improvements are the result of corrections to the velocity field in the geodynamo model.

Key words: Numerical solutions; Inverse theory; Dynamo: theories and simulations.

1 INTRODUCTION

The Earth's magnetic field was first noticed nearly 5000 yr ago (Roberts 1992), and it has been regularly recorded for the past 400 yr (Jackson *et al.* 2000). Knowledge of the origin, that is via convection in the outer core (geodynamo) has only existed for the last 100 yr, and the capability to numerically reproduce 'Earth-like' time varying magnetic fields for about 20 yr (Glatzmaier & Roberts 1995; Kuang & Bloxham 1997).

It is only natural to compare this evolution of awareness and knowledge to that of the weather patterns within the Earth's atmosphere. Certainly mankind have been aware of the importance of the weather since pre-historic times, and the need to forecast changes in weather has existed since the invention of agriculture. The science of weather prediction began in the nineteenth century with the introduction of weather maps, and numerical weather prediction (NWP) was proposed long before the advent of computers made it feasible (Richardson 1922). But once early computers came into being, research into NWP began in earnest. Charney (1949) worked out some of the computational issues by introducing the use of a quasi-geostrophic model, followed by the first successful 1-d numerical forecast using a barotropic model (Charney *et al.* 1950). The problem of how to initialize these forecasts was addressed by Bergthorsson & Döös (1955) and Cressman (1959), who developed the observation operator approach. This is a method that interpolates the state of the system to the location of the observations, which allows the difference between the observation and model output to be calculated. This difference can then be interpolated back to the computational grid in order to correct the model output and obtain an improved estimate of the state to be used as the initial condition

for the forecast computation, generally known as the analysis. Detailed accounts of the early years of NWP can be found in Kalnay (2003).

The point of introducing NWP here is that in these early years models were extremely primitive, lacking even a vertical dimension. It was many years before reliable forecasts could be extended beyond 1 d. The 2-d forecast from the European Centre for Medium Range Forecasts (ECMWF) in 1990 were roughly as good as the 1 d forecasts in 1966 (Houghton 1991). But the process that made this slow but steady improvement take place was the continued confrontation of observations and models over this time. When forecasts are compared with observations on a regular basis, specific problems with models can be identified and solved. Atmospheric modelling has greatly benefited by the process of confronting forecasts with real data because we can directly determine whether a change to a model produces an improved forecast.

Geodynamo modelling is most certainly more advanced than the 2-D atmospheric models used in the first weather forecasts. However, there is some disagreement as to whether they are yet good enough to make any kind of geomagnetic forecasts. For example, Glatzmaier (2002), points out a number of weaknesses in recent models. These include the fact that the models are as yet unable to operate anywhere near the physical parameter space of the Earth's core, due to the fact that these models are essentially direct numerical simulation (DNS) of the governing equations with added hyper-diffusivity. This is a major difference from atmospheric models, which make no attempt at DNS. Rather, they include substantial modelling of subgrid physical processes, including the planetary boundary layer (PBL) and cloud physics. He also points out that, while different geodynamo models give somewhat similar qualitative looking geomagnetic fields at the core–mantle boundary (CMB), the internal flow structures that produce these CMB fields can be quite different (Kuang & Bloxham 1997). Dormy *et al.* (2008), describe the relationship between the Rayleigh numbers ($R_{\rm th}$) and Ekman numbers (E) that can produce dynamo action, even when they are both far form the correct values for the core. Although recent scaling studies of numerical dynamo solutions, that is Christensen *et al.* (2010), indicate possibilities of extracting 'Earth-like' geodynamo solutions from current numerical simulations, the question remains as to which set of computationally realizable parameters produce the most earth like dynamo solutions. We argue that, like weather forecasting, geomagnetic forecasting can be used as a means to obtain the best possible parameter combinations, and help make further improvements to geodynamo models.

Forecasting of the Earth's geomagnetic field is as yet still in it's very early stages of development. For example, only the most recent International Geomagnetic Reference Field (IGRF) included a candidate secular variation (SV) model derived from a geodynamo model that assimilates geomagnetic observations (Finlay *et al.* 2010; Kuang *et al* 2010). This model predicts the SV Gauss coefficients up to degree 8 for the period from 2009.5 to 2015.0, and is the first opportunity to determine what contribution geomagnetic data assimilation can make to improving geomagnetic forecasts.

The most appropriate approach for making geomagnetic forecasts is a statistically based data assimilation system. Data assimilation is the method currently used in NWP to produce initial conditions for 5–10 d weather forecasts. It involves the collection of a large number of observations of atmospheric variables and comparing them to the forecast for the current state of the atmosphere. The differences between observation and forecast ($O - F$) are then used to make a correction to the forecast in order to produce a new, and hopefully more accurate, estimate of the current state, called the analysis. The analysis is then used as the initial condition for the next forecast run. The statistical aspect of the assimilation comes from the fact that neither the forecast or observations are perfect, and some estimate of their errors must be included in the assimilation process.

Data assimilation is generally categorized as sequential (Lorenc 1981; Lorenc 1986; Cohn 1997) or variational (Talagrand & Courtier 1987). The former involves assimilating all available observations near each assimilation time in order to obtain a minimum variance estimate of the analysis state. The latter assimilates all available observations over a time window so as to produce the minimum variance estimate over the entire time window.

Recently there have been research efforts towards applying data assimilation to geodynamo models and surface geomagnetic observations. One of the major obstacles to geomagnetic data assimilation is the limited observational record, in both and time and space. Only the poloidal component of the geomagnetic field is observable at the surface, and the observation record is only about 400 yr (not including archeo- and palaeomagnetic observations). Thus, initial investigations have focused on how much impact the surface observations can have on other state variables. Sun *et al.* (2007) and Fournier *et al.* (2007) used 1-D models of a coupled velocity and magnetic fields, and found that that limited magnetic observations have the potential to improve estimates of the velocity field when using an ensemble based sequential algorithm. The first assimilation system using a full geodynamo model was developed by Kuang *et al.* (2008). This system was used to carry out a series of Observing System Simulation Experiments (OSSEs), which demonstrated that synthetically generated surface observations of the poloidal magnetic field could be used to improve estimates of the state of the outer core (Liu *et al.* 2007). The first assimilation of real geomagnetic observations into a geodynamo model (Kuang *et al.* 2009) showed that even a short (100 yr) experiment could result in improvements in the surface geomagnetic forecast and begin to change the core flow near the CMB. Li *et al.* (2011), have also developed a variational data assimilation system with the potential to handle real geomagnetic observations. For a summary of some of the earlier work (see Fournier *et al.* 2010).

But we can only know whether a model estimate of the core flow has been improved by the assimilation using OSSEs, since the entire 'true' state of the core is then known exactly. Fournier *et al.* (2013) has conducted OSSE experiments using a perfect model (identical twin experiments), where the synthetic observations were created using the same model as the assimilation system. They used an existing ensemble Kalman filter framework (Nerger & Hiller 2013) combined with a geodynamo model (Dormy *et al.* 1998) and showed that this system can reproduce the core flow in a 'moderate' geodynamo after about 1000 yr of assimilation when there is no model error. The success of this approach is due to the estimate of the error correlation between the observed geomagnetic field and the velocity field, which enables the assimilation system to make corrections to the latter at each assimilation time. Ultimately, the most important verification of the success of geomagnetic data assimilation will come from improvements to forecasting of the geomagnetic field using real geomagnetic observations.

In this paper, we address three types of geodynamo and geomagnetic parameters: the Rayleigh number, the geomagnetic forecast error correlation length scale and the observation error estimate. These represent three very different aspects of geomagnetism. The Rayleigh number is a model parameter that gives an indication of the strength of heat generation within the core, the error correlation length scale controls how deeply the assimilation with spread

information from the geomagnetic observations into the core, and the observation error controls how much weight we give to each coefficient from the geomagnetic field model. Accurate knowledge of each of these is essential to the success of the assimilation system, and improved estimates of them will aid us in understanding the dynamics of Earth's core flows.

2 ASSIMILATION SYSTEM

We describe briefly the mathematics and common notation of sequential data assimilation algorithms (we refer the reader to Cohn 1997, for the details). Let $\mathbf{x}$ be the state vector of the physical system in consideration, $\mathbf{x}^f$ the forecast (model output), $\mathbf{x}^t$ the (unknown) true state. Observations, $\mathbf{y}$, are related to the true state by

$$\mathbf{y} = \mathbf{H}\mathbf{x}^t + \mathbf{z}^o, \tag{1}$$

where $\mathbf{H}$ is the observation operator, which projects the state vector onto the observation space. $\mathbf{z}^o$ is the observation error, and is generally treated as a zero mean Gaussian noise process. The observation error covariance is defined as

$$\mathbf{R} = \langle \mathbf{z}\mathbf{z}^T \rangle. \tag{2}$$

At a given time t_a when the observation $\mathbf{y}$ is made, the analysis $\mathbf{x}^a$ is determined from

$$\mathbf{x}^a(t_a) \;=\; \mathbf{x}^f(t_a) \;+\; \mathbf{K}\left[\mathbf{y} - \mathbf{H}\mathbf{x}^f(t_a)\right], \tag{3}$$

where $\mathbf{K}$ is the gain matrix, and $\mathbf{x}^f$ is the model output at t_a. In general, both $\mathbf{K}$ and $\mathbf{H}$ are time dependent. The analysis $\mathbf{x}^a$ is then used as the initial state for the forward model starting from t_a and onward until the next observation time $t_a + \delta t_a$. The assimilation process (3) is repeated at the new observation time.

The goal of this approach is that through the sequential assimilation of observations, the analysis $\mathbf{x}^a$ is expected to be a better estimate of the true state, which in turn is a better initial state for the next model run, producing and improved forecast. The observation operator $\mathbf{H}$ is defined by the location of the observed quantities and their relationship to the state variables (see Liu *et al.* 2007, for details). The gain matrix $\mathbf{K}$ is determined through the minimization of the estimated analysis error variance. Given estimates of the forecast error covariance, $\mathbf{P}^f$, and the observation error covariance, $\mathbf{R}$, the minimum variance analysis estimate can be obtained as

$$\mathbf{K} = \mathbf{P}^f\mathbf{H}^T\left[\mathbf{H}\mathbf{P}^f\mathbf{H}^T + \mathbf{R}\right]^{-1} \tag{4}$$

the forecast error covariance can be obtained from an ensemble of numerical model runs with Gaussian distributed perturbations to the initial states (Sun *et al*. 2007; Fournier *et al*. 2013). This approach is substantially more computationally expensive than modelled errors and gain matrix, as is used in optimal interpolation (OI). That is, OI is simply the assimilation algorithm described above with error covariances that are fixed in time (see Lorenc 1981, for a detailed description). The OI scheme employed in this paper has the advantage of reduced computational costs, and while it is not in fact 'optimal' (due to the imperfect knowledge of error statistics), it does allow us to focus on the response of the numerical dynamo model using different model and error parameters. This tuning helps to increase our knowledge of model errors and their sensitivity to changes different model parameters.

In order to derive the particular form of the gain matrix for geomagnetic data assimilation, we need to first understand the structure of the state vector from the forecast $\mathbf{x}^f$ and the observations $\mathbf{z}^o$. Because both of these are computed in spectral space, it is most convenient to compute (4) in spectral space as well.

The numerical model used in the geomagnetic data assimilation is the MoSST core dynamics model. We discuss here in detail only the magnetic field part of the model, so for complete details (such as the boundary conditions, etc.) see Kuang & Bloxham (1999). In this model, the state variables include fluid velocity field $\mathbf{v}$, the magnetic field $\mathbf{B}$ and the density perturbation Θ. $\mathbf{v}$ and $\mathbf{B}$ can each be described by poloidal and toroidal scalars, making five scalars for the physical state in the core. For example,

$$\mathbf{B} \;=\; \nabla\times(T_b\hat{\mathbf{r}}) \;+\; \nabla\times\nabla\times(P_b\hat{\mathbf{r}}) \;\equiv\; \mathbf{B}_T \;+\; \mathbf{B}_P\,, \tag{5}$$

where $\hat{\mathbf{r}}$ is the radial unit vector, T_b and P_b are the toroidal and poloidal scalars of the magnetic field, respectively. $\mathbf{B}_T$ and $\mathbf{B}_P$ in (5) are often called the toroidal field and the poloidal field, respectively. In the model, all scalar fields are expanded in spherical harmonic series, given radial position r. For example,

$$\begin{bmatrix} P_b \\ T_b \end{bmatrix} \;=\; \sum_{m=0}^{M}\sum_{l=m}^{L}\begin{bmatrix} b_l^m(r,t) \\ j_l^m(r,t) \end{bmatrix} Y_l^m(\theta,\phi) \;+\; C.C.\,, \tag{6}$$

where $\{Y_l^m\}$ are fully normalized spherical harmonic functions, $C.C.$ denotes the complex conjugate part, and (r, θ, ϕ) define the spherical coordinate fixed to the solid mantle. The spectral coefficients $\{b_l^m, j_l^m\}$ are defined on discrete radial grid points $\{r_i | i = 0, 1, \ldots N\}$ in the model.

To simplify the description, we denote by $\mathbf{x}_b$ the vector of all coefficients of the magnetic field

$$\mathbf{x}_b \;\equiv\; \left[b_l^m(r_i),\, j_l^m(r_i)\right]^T\;; \tag{7}$$

and similarly, $\mathbf{x}_v$ and $\mathbf{x}_\rho$ for those of the velocity field $\mathbf{v}$ and the density perturbation Θ, respectively. Therefore,

$$\mathbf{x} \;\equiv\; \left[\mathbf{x}_b, \mathbf{x}_v, \mathbf{x}_\rho\right]^T\,. \tag{8}$$

In the MoSST core dynamics model, the solid mantle is divided into two parts: a weakly conducting D'' layer in

$$1 \le r \le r_{do}$$

with the magnetic diffusivity η_{do} (scaled by that of the fluid outer core), and an electrically insulating upper mantle

$$r_{do} \le r \le r_{eo}.$$

r_{do} and r_{eo} are the mean radii of the top of the D''-layer and of the Earth's surface scaled by the mean radius of the CMB, respectively. In the insulating mantle and at the Earth's surface, the magnetic field is a potential field

$$\mathbf{B}_T \;=\; 0, \quad \mathbf{B}_P \;=\; -\nabla\psi, \tag{9}$$

where ψ is the potential scalar and satisfies the Laplace equation

$$\nabla^2\psi \;=\; 0\,. \tag{10}$$

By (5)–(9) and that the spectral coefficients are finite at infinity, we have

$$\psi = \sum_{l,m}\frac{c_l^m}{r^{l+1}}\,Y_l^m + C.C., \tag{11}$$

where c_l^m are constants. By the definitions (5), (6), (9) and (11), we can find that

$$b_l^m(r) \;=\; \frac{c_l^m}{l r^l} \;=\; \left(\frac{r_{eo}}{r}\right)^l b_l^m(r_{eo}) \tag{12}$$

in the solid mantle. In addition,

$$\frac{\partial}{\partial r} b_l^m \equiv b_l'^m = -\frac{l}{r} b_l^m . \tag{13}$$

Eq. (9) implies that, only the poloidal field coefficients $b_l^m(r_{eo})$ at the Earth's surface can be observed. They can then be continued downward to the top of the D'' layer via (12).

However, because of crustal magnetization, only a subset (with the degree $l \leq L_{\rm obs}$) can be extracted from the surface (or near surface) observations. At best, satellite observations can resolve up to $L_{\rm obs} = 14$ for the geomagnetic field (Langel & Estes 1982), and $L_{\rm obs}$ is smaller for pre-satellite eras because of the lower quality and sparse ground observation sites. Therefore, at the top of the D'' layer r_{do}, the observations are

$$b_l^{m(o)}(r_{do}) \equiv \left(\frac{r_{eo}}{r_{do}}\right)^l b_l^{m(o)}(r_{eo}) \quad \text{for} \quad l \leq L_{\rm obs}\,, \tag{14}$$

where the superscript '(o)' indicates the coefficients from observations.

In our system, both model and observation errors are included. Because of the large differences between the physical parameters obtainable in the geodynamo model and those appropriate for the Earth's core, large forecast error growth is expected between assimilation times. Thus, for the 20 yr analysis intervals used in this study, we expect that the forecast errors would remain much larger than the observation errors.

Estimates of uncertainty in geomagnetic observations have traditionally been limited (see Licht *et al.* 2013, for recent advances), so we use a simple observation error model that in which the errors are a fixed percentage of the spectral coefficient magnitudes. Thus the observation error covariance, $\mathbf{R}$, is modelled as a diagonal matrix in spectral space with elements:

$$\{R_{(lm),(l'm')}\} = (\sigma^o{}_{lm})^2 \delta_{ll'} \delta_{mm'}. \tag{15}$$

The observation error standard deviation is then modelled as:

$$\sigma^o{}_{lm} = \alpha^o \| b_l^{m(o)} \|, \tag{16}$$

where α^o, the observation error factor, is a real scalar coefficient between 0 and 1. Obviously this model does not reflect the improvements to measurement accuracy in past years, and the decrease in accuracy with the spherical harmonic degrees. We can, however, learn the sensitivity of the assimilation to the observation errors. This can help us to understand how future improvements to error estimates will help to improve geomagnetic forecasting and data assimilation. This observation model is less than ideal in other ways as well. For example, if the magnitude of a spectral coefficent becomes zero, the resulting error estimate would be zero. This is certainly incorrect, but our purpose is to show the impact of changes to observation errors on forecast accuracy. This should eventually lead to more reasonable error estimates for field model coefficients used in the assimilation, particularly when we start to use errors provided with geomagnetic field models.

The forecast error covariance ($\mathbf{P}^f$) is diagonal in the spectral space

$$\mathbf{P}^f_{(lm),(l'm')} = \mathbf{P}^{f(lm)} \delta_{ll'} \delta_{mm'}. \tag{17}$$

For a given l and m, its matrix elements are defined as:

$$\{P_{ij}^{f(lm)}\} = \rho_{ij} \sigma^f{}_i \sigma^f{}_j, \tag{18}$$

where i, j are the grid point locations in the radial direction), σ_i^f is the forecast error standard deviation at radial location r_i and ρ_{ij} is the forecast error correlation between the locations r_i and r_j.

The forecast error covariance is modelled by noting that the forecast errors will most likely be smallest near the CMB (where the impact of the observations is largest). Deeper in the core, the impact of the observations will be less (due to a decrease in error correlation), and we expect the forecast error to increase. The forecast also needs to satisfy the boundary condition at the top of the D$''$ layer

$$\frac{\partial b_l^m}{\partial r} = -\frac{l}{r_{dp}} b_l^m, \tag{19}$$

which results from the potential field structure of the magnetic field within the mantle (9).

One possible error covariance model which satisfies 19 has a radial error correlation of

$$\rho(r) = \mathrm{e}^{-(r_{dp}-r)^2/\Delta_c^2}, \tag{20}$$

and a forecast error standard deviation distribution,

$$\sigma^f(r) = \| b_m^l\,(r_{dp}) \| \left[r_{dp} + (r_{dp} - r) \right], \tag{21}$$

where r and Δ_c (the error correlation length scale) are normalized with the mean CMB radius, and $b_m^l(r_{dp})$ is the poloidal magnetic coefficient field at the top of the D''-layer. The resulting radial error covariance for an observation at the CMB is shown in Fig. 1, normalized by the forecast error variance at the CMB and for the case with Δ_c set to 70 per cent of the outer core. The peak covariance

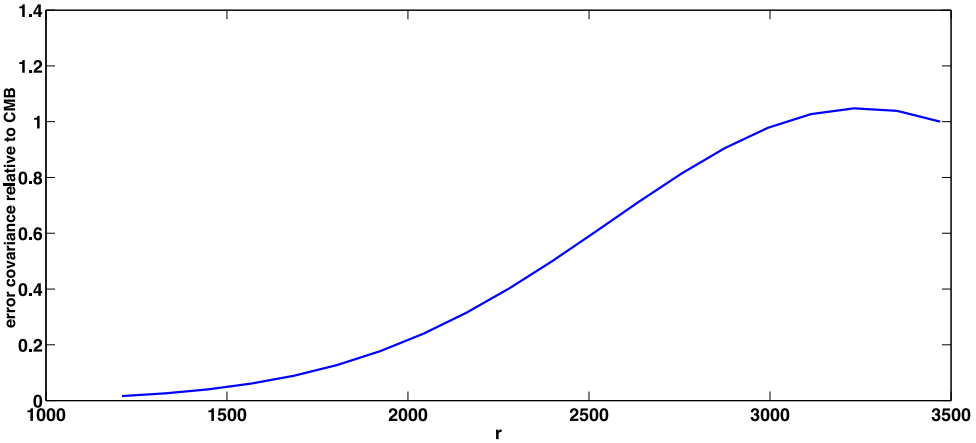

Figure 1. Radial dependence of the forecast error covariance between the CMB and points within the core, normalized by the error variance at the CMB ($\mathbf{P}^f/\sigma^2_{\rm cmb}$).

occurs about 300 km below the CMB, which is a result of the increasing error variance with depth. This is where the impact of the observations is largest for this value of Δ_c.

While Δ_c is not explicitly known, it can be used as a tuning parameter by running the assimilation system with different values. Comparisons of the forecast error for each value of Δ_c are a good indication of the optimal error correlation length scale. In the next section, we describe a series of experiments using this system in order to gain a better understanding of how the model and assimilation system responds to changes in both model and assimilation parameters. In particular, we will focus on the Rayleigh number, the radial error correlation length scale and the observation errors.

3 RESULTS

We have used the geomagnetic data assimilation system described in the last section to carry out a number of experiments with the goal of understanding the sensitivity of the forecast accuracy. The initial state (forecast) used for the assimilation is obtained from well developed dynamo solutions of the simulation with the same model parameters that are used in the assimilation. The assimilation in each experiment starts in the year 1590 and continues to to 1990. The observations used are from the field models GUFM1 (Jackson *et al.* 2000) for the period 1590–1960, and CM4 (Sabaka *et al.* 2004) for 1960–1990.

These field models do not provide error estimates associated with the Gauss coefficients. However, it is expected that the errors become larger further back in time. The significant early events that had an impact on the accuracy of the data include the substantial increase in the density of global ship data between 1590 and 1750, the widespread use of the Harrison chronometer in the 1780s and the measurement of absolute intensity after 1832. Permanent observatory data became available in the 19th century with increasing density up until the satellite era, which began in 1965 with Polar Orbiting Geophysical Observatories (POGO), Magnetic Field Satellite (MAGSAT) in 1980, Ørsted in 1999 and Challenging Minisatellite Payload (CHAMP) in 2000. Each increase of measurement data has resulted in improvements in field models since 18th century. But we still lack quantitative measures of how their accuracy changes in time. Therefore, one objective of our study is to use data assimilation approach to learn how different observation accuracies impact the assimilation.

Much of the analysis done in this paper relies on comparisons between the geodynamo model forecasts and the field models (which are used as observations in this work), and lack of knowledge of field model errors makes the task of assessing the success of the assimilation system more difficult. The observed minus forecast ($O - F$) fields are generally used as an indication of the accuracy of the forecast, but this assumes that there is some consistent accuracy of the observations, which is not the case here since observation uncertainty varies with degree and time. The variance of the ($O - F$) for a single coefficient at the CMB is defined as:

$$(\sigma^2_{omf})^l_m = \left\langle \left| (b^l_m)^o - (b^l_m)^f \right|^2 \right\rangle. \tag{22}$$

If we assume that the forecast and observation errors are uncorrelated (this is often a good approximation in assimilation systems), then we can decompose the variance of the ($O - F$) in terms of the forecast and observation errors:

$$\begin{aligned}(\sigma^2_{omf})^l_m &= \left\langle \left| (b^l_m)^o - (b^l_m)^t + (b^l_m)^t - (b^l_m)^f \right|^2 \right\rangle \\ &= (\sigma^2_o)^l_m + (\sigma^2_f)^l_m,\end{aligned} \tag{23}$$

where $(b^l_m)^t$ are the unknown true poloidal field coefficients at the CMB. Thus the variance of the ($O - F$s) are a combination of observation and forecast error. It is not desirable to draw the model output too close to the observations, since this would result in including observation errors in the analysis.

3.1 Forecast error correlation length scale, Δ_c

The first set of experiments involves different values for Δ_c, which controls how deep within the core the forecast errors are correlated. For these experiments we used model parameters of $R_{\rm th} = 7.5R^c$, $E = 5 \times 10^{-6}$; and observation error parameter of $\alpha^o = 0.001$ (so that the observation error estimate is much smaller than the forecast error). Runs were done for Δ_c varying from 0.1 to 0.9 in increments of 0.1, and we calculate the rms of the ($O - F$):

$$\mathrm{rms}(O-F) = \left[\sum_{l=1}^{8} \sum_{m=0}^{l} l^2(l+1)^2 [(b^m_l)^o - (b^m_l)^f]^2 \right]^{1/2}. \tag{24}$$

It is also useful to show the rms of the cumulative ($O - F$), which at any given time is the sum of the ($O - F$) since the beginning of the assimilation run. This gives an indication of the bias between the observation and forecast, since random difference should average out over a long time. It can be calculated from

$$(O-F)_{\rm cumulative} = \frac{1}{n} \sum_{i=1}^{n} \left[(b^m_l)^o - (b^m_l)^f \right]_i, \tag{25}$$

where n is the number of forecast times from the start of the assimilation to the current time. The cumulative ($O - F$) can then be used to calculate and rms as a function of time using (24). The cumulative ($O - F$) was initially used by Dee & da Silva (1998) as a method to estimate model error. Aubert & Fournier (2011) demonstrated its use in geomagnetic data assimilation in a series of twin experiments in which synthetic observations are generated by the same model as is used in the assimilation. In this perfect model scenario, the rms of the cumulative ($O - F$s) where shown to decay in time. In this work, we expect significant model errors due to the limitations on the dynamo parameters. But the differences in cumulative ($O - F$s) give a clear indication of what set of model parameters results in the smallest model error. We present all of the results in terms of scaled (i.e. non-dimensional) variables since we wish to focus on relative differences. This gives a clearer picture of the relative success of the assimilation experiments.

Fig. 2 shows the rms ($O - F$) (a) and the rms cumulative ($O - F$) (b) for just the two extremes of these assimilation runs ($\Delta_c = 0.1$ and 0.9) for the period 1590–1990, which allows the differences to be seen more clearly. We plot here (and in all subsequent ($O - F$) plots) just the 20-yr forecasts right before the assimilation is done, so that what is shown is the maximum error for each 20-yr assimilation cycle. The $\Delta_c = 0.9$ case is seen to result in rms ($O - F$) differences that are about 10 per cent less than the $\Delta_c = 0.1$ case, indicating that for the model parameters described above, there is significant forecast error correlation throughout the outer core. This is the result of large bias or model error, which tend to result in long correlation distances. Panel b shows this more clearly, where the rms of the cumulative ($O - F$) is about 1/3 less for the $\Delta_c = 0.9$ case.

Decreases in the model error through model improvements (e.g. higher resolution or improvements to model parameters) should therefore result in lower error correlation length scales. This will

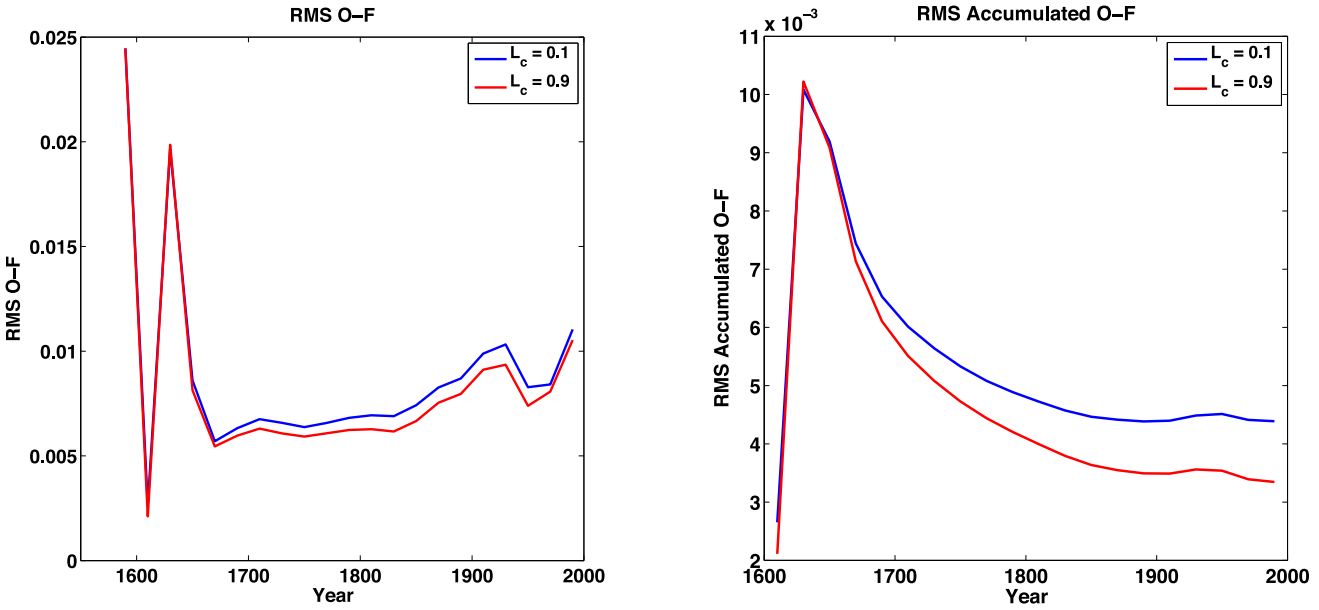

Figure 2. Rms $(O - F)$ versus time (a) and rms of cumulative $(O - F)$ versus time (b) for assimilation runs with $R_{\rm th} = 7.5R^c$, $E = 5 \times 10^{-6}$, $\alpha^o = 0.001$ and $\Delta_c = 0.1, 0.9$.

provide an additional means to test for reductions in model error in the assimilation system.

3.2 Rayleigh number, $R_{\rm th}$

Data assimilation is a particularly valuable tool for model parameter estimation. By varying a parameter in different assimilation runs, changes in the forecast accuracy can be used to determine an optimal set of parameters. For example, scaling rules (e.g. Christensen & Aubert 2006; Christensen *et al.* 2010) have been developed that identify ratios between Rayleigh and Rossby numbers that result in the most 'Earth like' magnetic fields. This is done using a set of structural and spectral properties of the geomagnetic field at the CMB and comparing them with those derived from various geomagnetic field models, for example CALS7K2 (Korte & Constable 2005), *gufm1* (Jackson *et al.* 2000) and IGRF11 (Finlay *et al.* 2010). For the Ekman numbers $E \geq 10^{-6}$, Christensen *et al.* (2010) identified the wedge of the magnetic Reynolds number R_m $(=UL/\eta$, where U and L are typical velocity and length scales of the core flow) in which the dynamo generated field has an acceptable morphology. The Ekman number used in this study is approximately equivalent to $E = 2 \times 10^{-5}$ in Christensen *et al.* (2010). And the lower and the upper bound for acceptable field morphology is $200 \leq R_m \leq 1000$.

An assimilation system can add additional quantitative information about the model parameters, and we would like to determine whether changing model parameters has any significant impact on the forecast. We have have run assimilation experiments with three different Rayleigh numbers $R_{\rm th} = 7.5R^c$, $15R^c$ and $30R^c$, which result in $R_m \approx 170$, 230 and 320, respectively. The first experiment is therefore below the lower boundary, the second is approximately on the lower boundary, and the third is within the compliant region. In all cases the forecast and observation error standard deviations used $\alpha^o = 0.01$, which means that the analyses give most of the weight to the observations. The forecast error covariance used an error correlation length scale of $\Delta_c = 0.7$. We are interested in determining which of these Rayleigh numbers produces the best 20-yr geomagnetic forecasts when run from 1590 to 1990, starting each from a long model run using their respective parameter values (E and $R_{\rm th}$). We have estimated dynamo timescales for each of these parameter combinations by calculating averages of the poloidal field divided by the poloidal secular variation:

$$\tau = \text{mean}\left(\frac{b_l^m}{\dot{b}_l^m}\right)$$

for a long model run, which allows us to separate out dipole and non-dipole timescales. For $R_{\rm th} \approx 7.5R^c$, we find $\tau_{dp} \approx 30\,000$ yr and $\tau_{ndp} \approx 3000$ yr; for $R_{\rm th} = 15R^c$, $\tau_{dp} = 3000$ yr and $\tau_{ndp} = 250$ yr; for $R_{\rm th} = 30R^c \tau_{dp} = 1000$ yr and $\tau_{ndp} = 100$ yr. Here τ_{dp} is the dipole timescale and τ_{ndp} is the non-dipole timescale. Thus for some of these parameter combinations, the timescales for the non-dipole field is on the same order as the data record that we are assimilating.

Fig. 3 shows the rms of the $(O - F)$ (a) and the cumulative $(O - F)$ (b) of the poloidal geomagnetic field at the CMB from 1590 to 1990. The first thing that stands out is that the rms of the $(O - F)$ (panel a) at the initial state is largest for $R_{\rm th} = 30R^c$, and that it decreases with $R_{\rm th}$. This may well be the result of the larger variability of the poloidal field at the CMB at larger Rayleigh numbers, which are initially unconstrained by observations. The rms $(O - F)$ decreases rapidly in each case, in part due to the small observation errors used in these experiments. The smallest rms difference at the end of the assimilation occurs for the $R_{\rm th} = 30R^c$ case. The cumulative $(O - F)$ (which does not include the initial time of 1590 since the observations have not yet been assimilated) shows more dramatic differences between the three experiments, with the $R_{\rm th} = 30R^c$ resulting in the lowest rms values at the end of the assimilation. The $R_{\rm th} = 7.5R^c$ is not only about four times larger, but there is an overall rise in the rms difference. This indicates subtantially higher model bias for this set of parameters.

These results are dependent on both the observation and forecast error models as well as the assimilation algorithm itself. Further parameter studies will investigate how all of these parameters interact and impact the accuracy of geomagnetic forecasts.

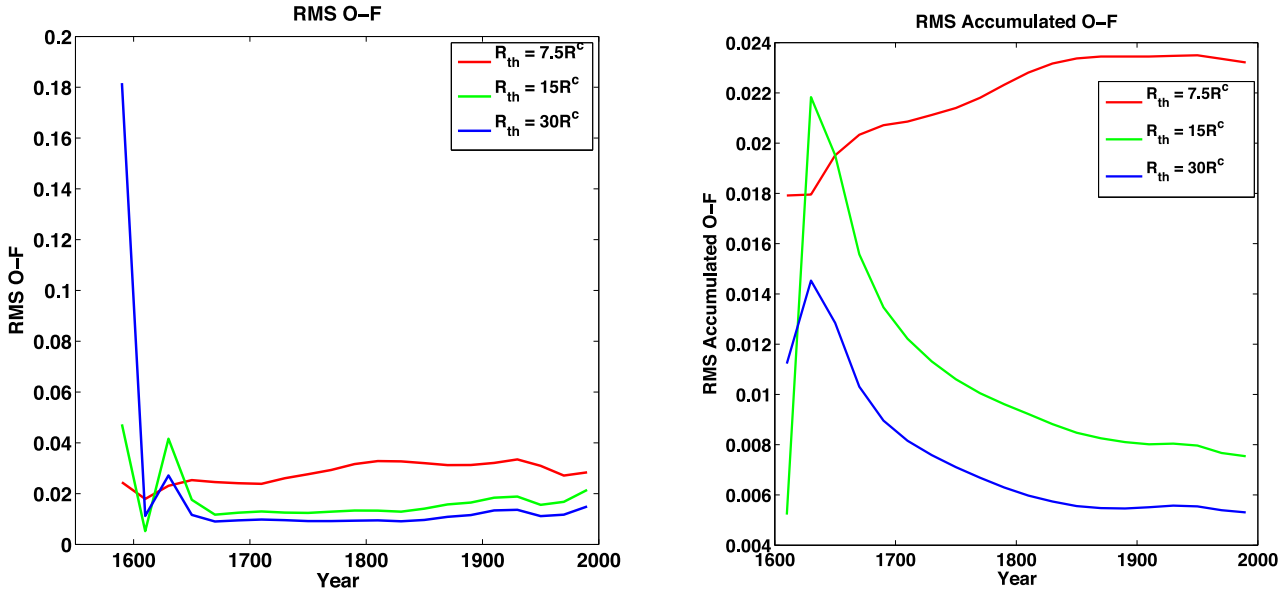

(a) (b)

Figure 3. Rms $(O - F)$ versus time (a) and the cumulative rms $(O - F)$ versus time (b) for assimilation runs with $E = 5 \times 10^{-6}$, $\alpha^o = 1.0$, $\alpha^o = 0.001$ and $\Delta_c = 0.7$. The Rayleigh numbers $R_{\rm th} = 7.5R^c$, $15R^c$ and $30R^c$.

3.3 Observation error factor α^o

In the experiments described above we have assumed that the observation errors, while not zero, are much smaller than the forecast errors for the poloidal magnetic field at the CMB. This may not be an optimal assumption. But it opens the door for developing some techniques to evaluate different error estimates for the geomagnetic observations being assimilated.

Finite observation error also points to a need for some care in using $(O - F$s) to evaluate the relative success of the assimilation. If the observation error is not accurately known, then it is difficult to use observations to determine forecast accuracy.

However, we do know that geomagnetic field models have become much more accurate in recent decades, and that lower spherical harmonic degrees are more accurate than higher degrees. It should be pointed out here that observation errors may be uniform across the spherical harmonic spectrum. But, considering that the magnitude of the Gauss coefficients decreases as the degree l increases, the errors relative to the Gauss coefficients (α^o) increases with l.

So the question remains: Is it always better with smaller $(O - F)$ values? The answer really depends upon how accurate the observations are. If the observation error is relatively large, it is probably better not to draw the model too close to the observations. In the meantime, sensitivity of forecasts can be also used to assess the significance of observation errors. We can demonstrate these by considering three experiments in which we vary the observation error factor α^o.

Fig. 4 shows the rms of the $(O - F$s) (a) and cumulative $(O - F$s) (b) from assimilation runs with α^o set to 0.001, 0.1 and 0.2. When $\alpha^o = 0.001$ (green), the analyses essentially set the poloidal magnetic field equal to the observed values at the CMB. Thus, the first 20-yr forecast in 1610 results in an rms difference that is about 10 times smaller than the initial difference. But at the next forecast time (1630) the error has increased nearly back to the initial value. Eventually these oscillations settle into a more stable set of forecasts starting in 1670, but the rms difference actually grows very gradually from this time forward until the final forecast in 1990. Thus the rms $(O - F)$ is actually larger in 1990 than it is in 1610, in spite of the fact that we believe that the field model is much more accurate in 1990. A likely scenario is that by giving too much weight to the observations in early years, observation errors are inserted into the analyses and are then propagated forward by the model. When $\alpha^o = 0.1$ (blue), the response is quite different. Now there is a gradual reduction in the rms difference between forecast and observation which reaches a minimum near the end of the assimilation. In fact the rms $(O - F)$ is almost identical to the $\alpha^o = 0.001$ case by 1970, and the larger differences early in the assimilation insure that observation errors are not being added into the analyses. The cumulative $(O - F$s) in panel (b) show that while the bias in the $\alpha^o = 0.001$ case is substantially lower than when $\alpha^o = 0.1$, the rms in the latter case is still declining significantly by the end of the assimilation run. A longer assimilation run could possibly show that the difference in bias in the 2 experiments is relatively insignificant.

Generally we would expect that a properly optimized assimilation system should show a gradual reduction in $(O - F)$ statistics as the model absorbs new observational information over time. The fact that the $\alpha^o = 0.001$ case shows an immediate drop in $(O - F)$ is because the assimilated data and the observations for comparing with the forecasts are from the same source, and because the 20-yr forecast period is a relatively short time to build up errors in a geodynamo model. A more objective comparison would be the difference with an outside observation that is not assimilated. For example, in atmospheric data assimilation, satellite observations are assimilated into a general circulation model (GCM) and statistical comparisons are made with *in situ* surface or aircraft data (e.g. Tangborn *et al.* 2013). If the assimilation is helping to improve the model output, then the differences between forecasts and the independent observations should be reduced, even if they are made far from the locations of the assimilated observations.

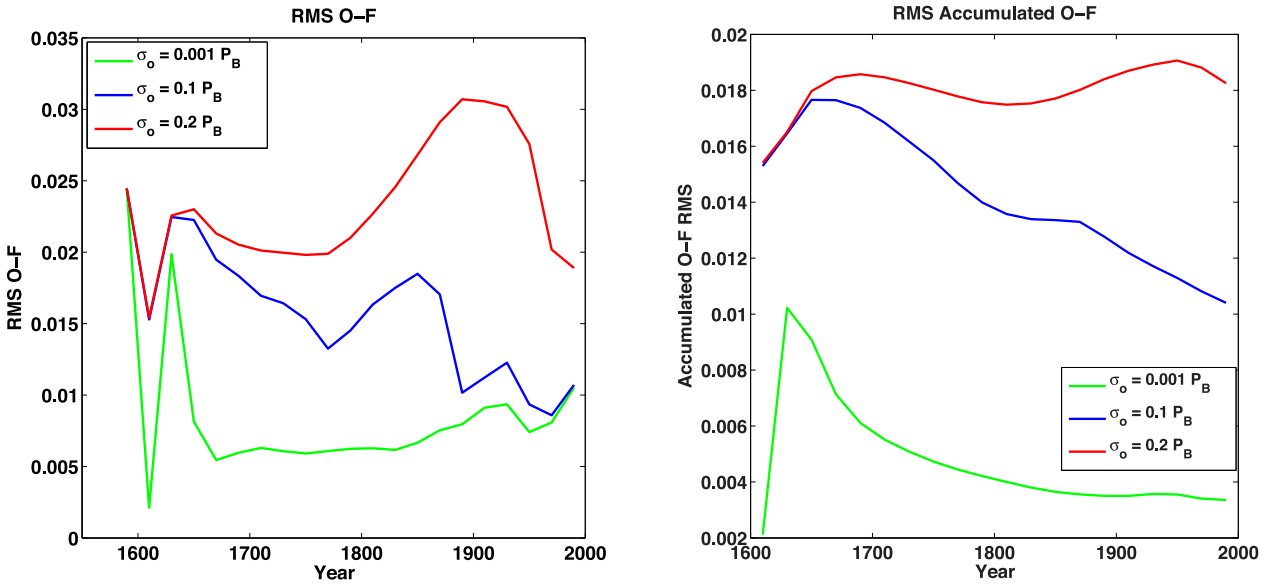

Figure 4. Rms $(O - F)$ versus time (a) and the cumulative rms $(O - F)$ versus time (b) for the assimilation runs with $R_{\rm th} = 7.5R^c$, $E = 5 \times 10^{-6}$, $\Delta_c = 0.7$ and $\alpha^o = 0.001$, 0.1 and 0.2.

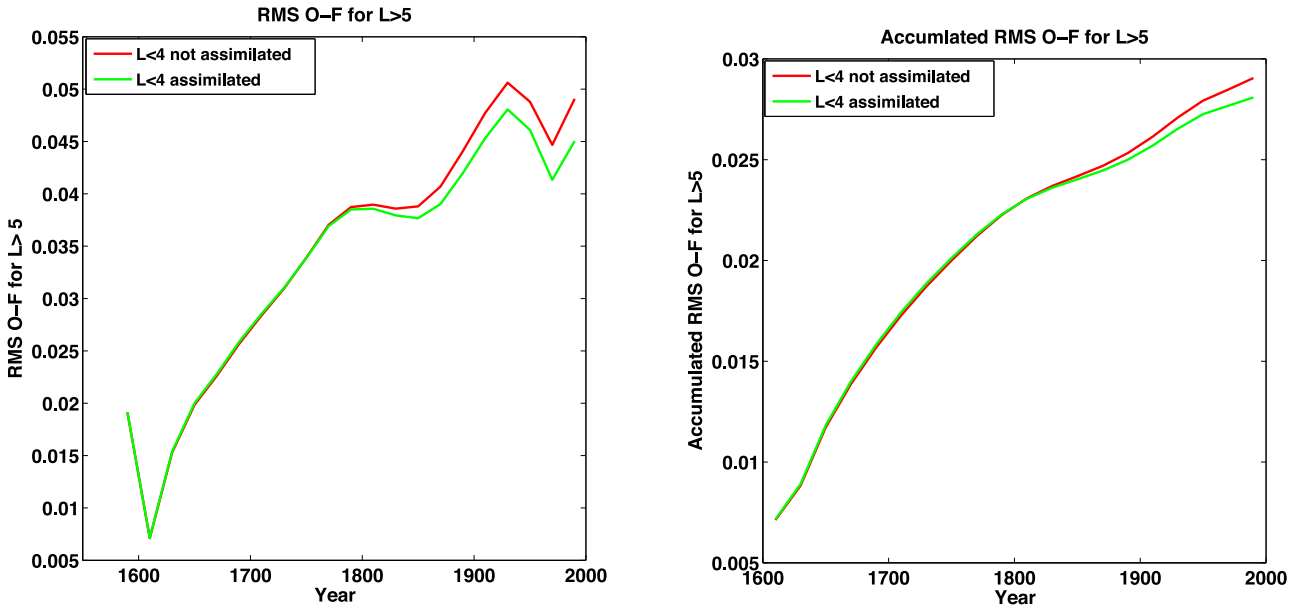

(a) (b)

Figure 5. Rms $(O - F)$ (a) and rms cumulative $(O - F)$ (b) for $l \geq 6$, as a function of time for assimilation runs with $R_{\rm th} = 15R^c$, $E = 5 \times 10^{-6}$, $\Delta_c = 0.7$. The observation error factor for $l > 3$ is $\alpha^o = 1.0$, while the errors for $l \leq 3$ are either $\alpha^o = 0.1$ (green) or ∞ (red).

In geomagnetic data assimilation, one might be able to create similar scenario by assimilating, for example, observatory data, and then comparing forecasts with, for example satellite data. But in many (but not all) of the field models, both types of data are utilized to obtain the Gauss coefficients.

In this work, we take an alternative approach: creating an outside data set by assimilating only a subset of the spectral coefficients. Then, the $(O - F)$ rms statistics should be calculated from only those coefficients that are not assimilated. For example, we can assimilate only the low degree coefficients ($l \leq 3$), and then calculate the rms $(O - F)$ for the unassimilated higher degree terms ($l > 3$). Improvements in the rms will then only occur if the model converts lower resolution data into higher resolution improvements in the forecast geomagnetic field. This is a more difficult improvement to make than moving information from one data source to the location of another measurement because the information needs to transfer through the non-linear terms in the momentum equation rather than material transport. We expect therefore that the impact of the assimilation will be much smaller.

We have conducted a number of experiments to determine whether this approach could be used to study the impact of assimilating either the low or high degrees of a geomagnetic field model. For the short (400 yr) assimilation runs in this study, we have found that high degree observation have little impact on low degrees (not

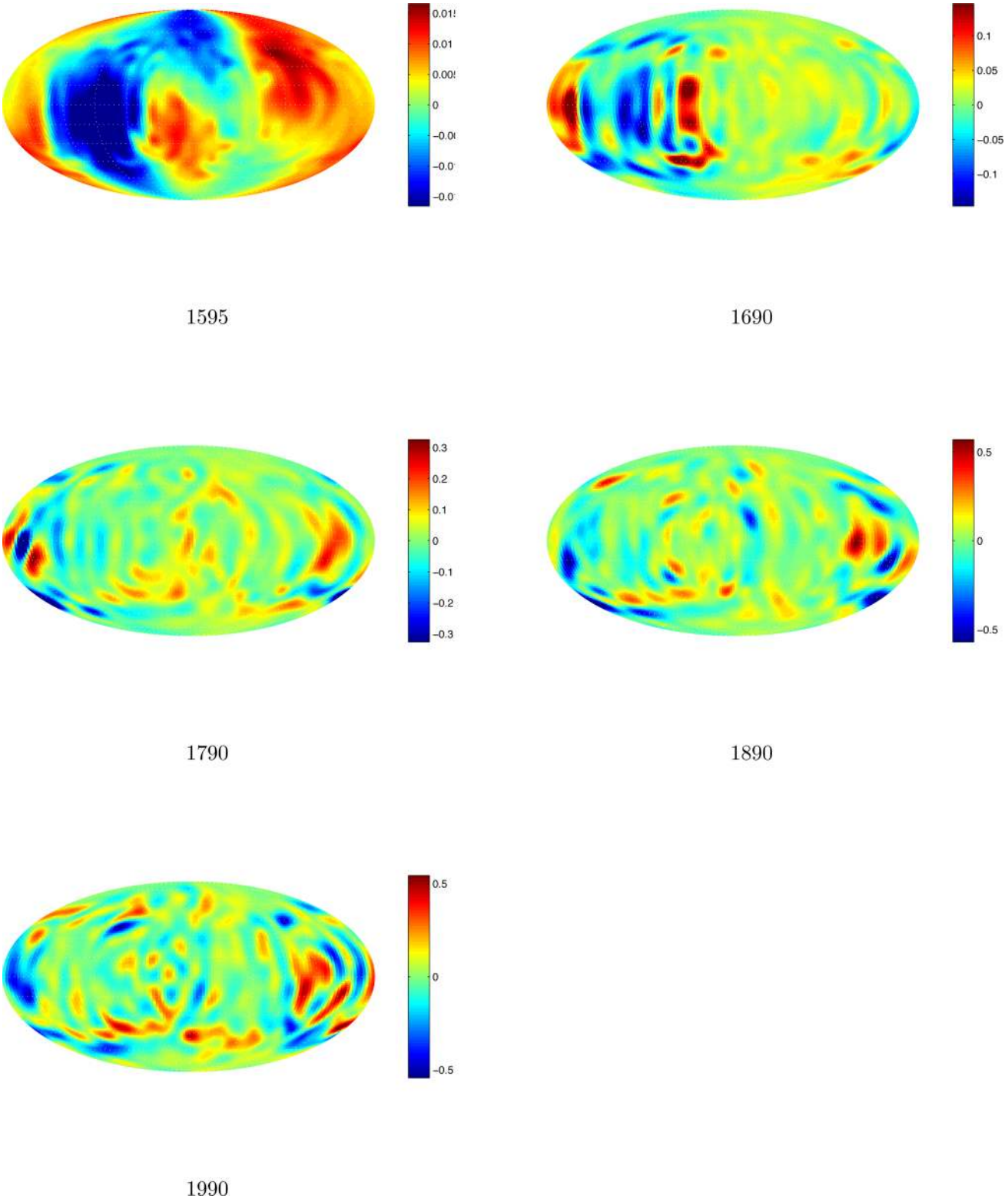

Figure 6. Difference in mid-core magnetic field with and without $l < 4$ observations assimilated (same experiment as Fig. 5), shown every 100 yr from 1595 to 1990.

shown). This may be due to the relatively low energy content of the higher degrees, or to the lower accuracy of the small scales. Assimilating large scale (low degree) coefficients, on the other hand, does have a positive impact on the accuracy of the small scale part of the forecast. For example, Fig. 5, shows the rms of the $(O - F)$ for higher degrees ($L > 5$) only for two experiments with (red curve, $\alpha^o = 0.1$) and without (green curve, $\alpha^o = \infty$) the lower degrees ($l \leq 3$) assimilated. In both cases the higher degrees are assimilated with a relatively large error estimate ($\alpha^o = 1.0$) so that they are only slightly constrained. Including the large scales in the assimilation

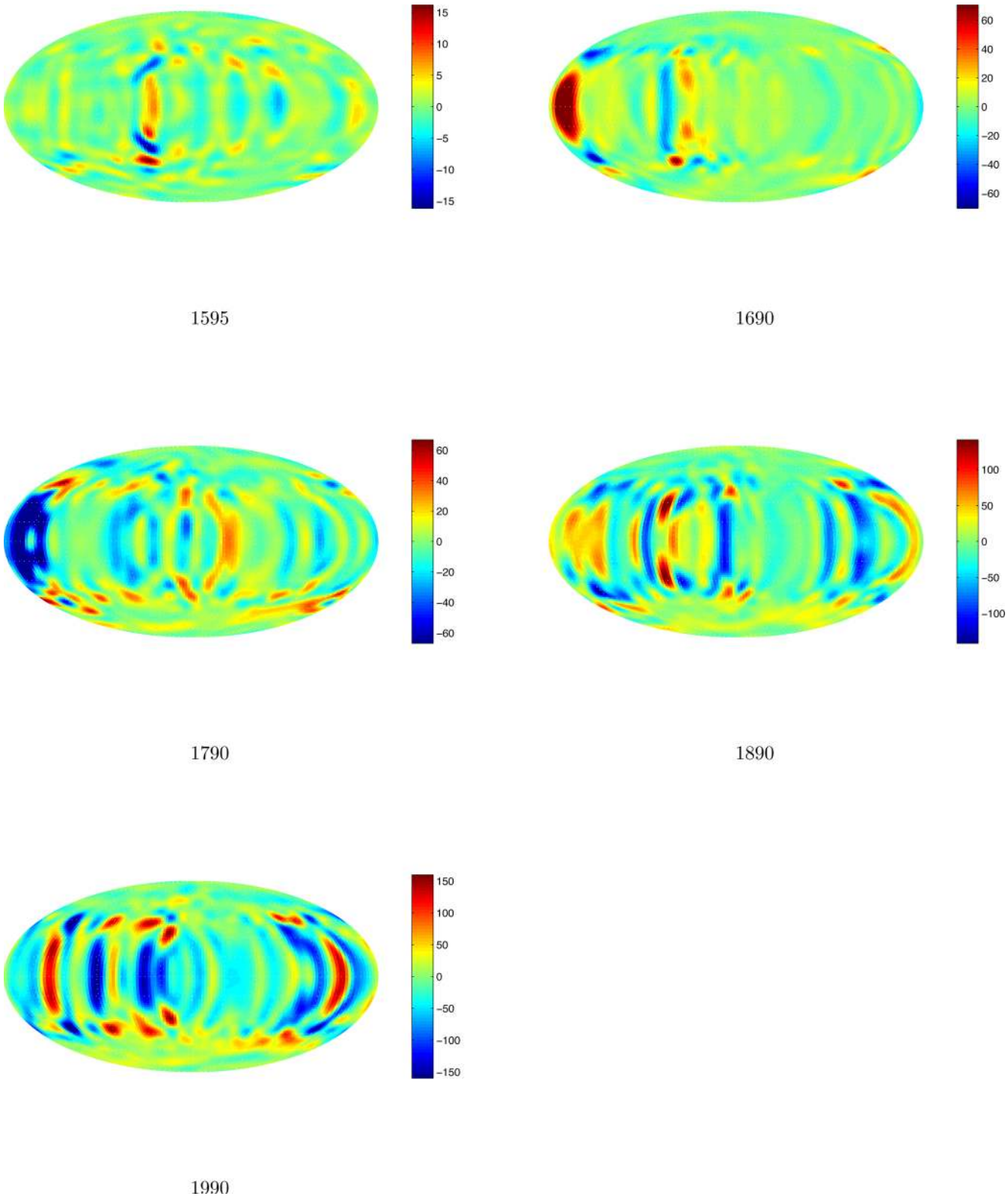

Figure 7. Difference in mid-core velocity field with and without $l < 4$ observations assimilated shown every 100 yr from 1595 to 1990.

is seen to have postive impact on the small scales, and the rms of the cumulative $(O - F)$ (Fig. 5b) shows that there is a systematic difference between the observations and forecast. This result is expected because the small scales are relatively unconstrained by the observations.

If we look at the core field differences (magnetic or velocity) between different assimilation runs, we can gain some insight on how low degree observational information is spread to the higher degrees. Fig. 6 shows the difference in the mid outer core magnetic field with and without the low degree coefficients assimilated

starting in 1595 (the initial differences in 1590 are zero) and ending in 1990. In 1595, the difference is global and is entirely at the largest scales because the only difference between the experiments is the weight given to the low degree observations. But by 1690 the differences begin to emphasize smaller scales, and this trend continues until the final time in 1990. Plots of the differences in the velocity field for the same two experiments (Fig. 7) demonstrate that the assimilation begins to effect the smaller scales within 5 yr, thus preceding the small scale differences in the magnetic field. This transfer from large scales to small scales can only happen through the core flow, since the momentum equation is the only fully non-linear term in the Navier–Stokes equation.

Figs 6 and 7 also show how the assimilation gradually alters the dynamo state through the interaction of the assimilation and model. Observations at the CMB are ingested into the system every 20 yr and directly affect only the poloidal magnetic field, primarily near the CMB. After each assimilation, the model is run forward in time, and the correction made to the poloidal field near the CMB is spread to other variables and other regions of the outer core through the interaction of the momentum, induction and energy equations. Thus we see only very small changes at the mid-outer core in 1595, but gradually much larger changes over the 400 yr of the numerical experiment. The changes in the magnetic field occur more rapidly, since this it is a directly observed variable. The velocity field changes more slowly, but continues to show significant changes through the experiment as information is passed by the model from the magnetic field to the velocity field.

4 CONCLUSIONS

This paper has presented a number of geomagnetic assimilation experiments for the period 1590–1990 in order to show how assimilation can be used to better understand several important model and observation parameters, including the Rayleigh number, forecast error correlation length scale and the observation uncertainty. This is done by comparing 20-yr forecasts with the observations from the geomagnetic field model and computing the rms difference. While we have not made an effort to determine the optimal values for any of these parameters, we have shown how assimilation can help to gain some insight on searching for better estimates.

The forecast error correlation length, Δ_c, is not a model parameter but rather an estimate of how much an observation at the CMB will affect the poloidal magnetic field deep within the core. We have done a series of experiments with varying Δ_c only for the lowest of the Rayleigh numbers used in this work ($R_{\rm th} = 7.5R_c$), and found that the most accurate forecasts were obtained when the errors at the CMB were essentially correlated with the errors at the inner core boundary (ICB). This result is dependent on other model parameters, but it provides a starting point for future assimilation experiments.

We also show that there is significant sensitivity to the magnetic Reynolds number (via the Rayleigh number in this study), with the most accurate forecasts achieved with a $R_m = 340$ (i.e. $R_{\rm th} = 30R_c$). This agrees well with the scaling rules of Christensen *et al.* (2010) because these parameters are within the compliant region that they have identified. This is only a first step in what is expected to be a computationally expensive study of parameter regimes in geomagnetism. A complete study of the impact of model parameters on geomagnetic forecast accuracy will involve variations in both E and $R_{\rm th}$, and significant changes to either will also require substantially higher model resolution and therefore a large increase in computational resources. But these requirements are rapidly becoming available for earth sciences research.

Finally, we have begun to examine how one might use data assimilation to gain further knowledge of the accuracy of geomagnetic observations. A comprehensive error analysis probably cannot be completed using data assimilation alone. There are too many coefficients, and the errors for each are changing in time. And simply drawing the geomagnetic forecast closer to an observation that we don't have an error estimate for is difficult to interpret. The fact that the measured core field is only a small fraction of that generated by the geodynamo, and that core flow is not directly observable, indicates both the complexities of and the need for these efforts. Our study here is to demonstrate that assimilation results (and thus forecast accuracies) are very sensitive to observation errors. This sensitivity could and should be exploited to gain further insight on error estimates.

If we set the observation error to be very small, the $(O - F\text{s})$ tend to quickly drop below the initial difference, but then show very little further decline. But since we know that the observations are more accurate later in time, it would be more realistic to see a more gradual decline in the $(O - F\text{s})$. The fact that we are using using geomagnetic field models (GFMs) as the geomagnetic observations complicates this aspect of the study. Because GFMs generally use all of the available measurements, we don't have an independent data set to compare with. We have shown that one possible solution to this issue is to assimilate only part of the GFM output (e.g. large scales only), and make the GFM comparisons with the unassimilated coefficients (small scales only). By varying the estimated observation errors, we see an impact on the unassimilated scales, which is an indication that should be possible to find optimal values. It would be particularly beneficial to combine this approach with some of the recent work on field models that include error estimates (Korte *et al.* 2011; Gillet *et al.* 2013; Licht *et al.* 2013). One could then start with the errors provided with these models, and make relatively small changes to verify or even refine the error estimates. This is an area of future research focus.

ACKNOWLEDGEMENTS

This work was funded by grants from NSF (EAR-0757880) and the NASA Earth Surface and Interiors program (NNX09AK 70G).

REFERENCES

Aubert, J. & Fournier, A., 2011. Inferring internal properties of Earths core dynamics and their evolution from surface observations and a numerical geodynamo model, *Nonlin. Process. Geophys.,* **18,** 657–674.

Bergthorsson, P. & Döös, B., 1955. Numerical weather map analysis, *Tellus*, 329–340.

Bloxham, J., Gubbins, D. & Jackson, A., 1989. Geomagnetic secular variation, *Phil. Trans. R. S. Lond. A,* **329,** 415–502.

Charney, J.G., 1949. On a physical basis for numerical prediction of large-scale motions in the atmosphere, *J. Meteor.,* **6,** 371–385.

Charney, J.G., Fjørtoft, R. & von Neuman, J., 1950. Numerical integration of the barotropic vorticity equation, *Tellus,* **2,** 237–254.

Christensen, U.R., 2010. Dynamo scaling laws and applications to the planets, *Space Sci. Rev.,* **152,** 565–590.

Christensen, U.R. & Aubert, J., 2006. Scaling properties of convection-driven dynamos in rotating spherical shells and application to planetary magnetic fields, *Geophys. J. Int.,* **166,** 97–114.

Cohn, S.E., 1997. An introduction to estimation theory, *J. Meteorol. Soc. Japan,* **75,** 257–288.

Cressman, G.P., 1959. An operational objective analysis scheme, *Mon. Wea. Rev.,* **87,** 367–374.

Dee, D.P. & da Silva, A.M., 1998. Data assimilation in the presence of forecast bias, *Q.J.R. Meteorol. Soc.*, **124,** 269–295.

Dormy, E., Cardin, P. & Jault, D., 1998. MHD flow in a slightly differentially rotating spherical shell, with conducting inner core, in a dipolar magnetic field, *Earth planet Sci. Lett.,* **160,** 15–30.

Dormy, E. & Le Mouël, J.-L., 2008. Geomagnetism and the dynamo: where do we stand?, *Comp. Rend. Phys.,* **9,** 711–720.

Finlay, C. *et al.*, 2010. International geomagnetic reference field: the eleventh generation, *Geophys. J. Int.,* **183**(3), 1216–1230.

Fournier, A., Eymin, C. & Alboussiere, T., 2007. A case for variational geomagnetic data assimilation: insights from a one-dimensional, nonlinear and sparsely observed MHD system, *Nonlin. Proc. Geophys.,* **14,** 163–180.

Fournier, A. *et al.*, 2010. An introduction to data assimilation and predictability in geomagnetism, *Space Sci. Rev.,* **155,** 247–291.

Fournier, A., Nerger, L. & Auber, J., 2013. An ensemble Kalman filter for the time-dependent analysis of the geomagnetic field, *Geochem. Geophys. Geosyst.,* **14**(10), 4035–4043.

Gillet, N., Jault, D., Finlay, C.C. & Olsen, N., 2013. Stochastic modeling of the Earth's magnetic field: inversion for covariances over the observatory era, *Geochem. Geophys. Geosyst.*, **14,** 766–786.

Glatzmaier, G.A., 2002. Geodynamo simulations—how realistic are they?, *Annu. Rev. Earth planet. Sci.,* **30,** 237–257.

Glatzmaier, G.A. & Roberts, P.H., 1995. A three-dimensional convective dynamo solution with rotating and finitely conducting inner core and mantle, *Phys. Earth planet. Inter.,* **91,** 63–75.

Houghton, J., 1991. The Bakerian Lecture 1991. The Predictability of Weather and Climate, *Phil. Trans.: Phys. Sci. Eng.,* **337,** 521–572.

Jackson, A., Jonkers, A.R.T. & Walker, M.R., 2000. Four centuries of geomagnetic secular variation from historical records, *Phil. Trans.: Math., Phys. Eng. Sci.,* **358,** 957–990.

Kalnay, E., 2003. *Atmospheric Modeling, Data Assimilation and Predictability*, Cambridge Univ. Press.

Korte, M. & Constable, C.G., 2005. Continuous geomagnetic field models for the past 7 millennia: 2. CALS7K. *Geochem. Geophys. Geosyst.,* **6,** Q02H16, doi:10.1029/2004GC000801.

Korte, M., Constable, C., Donadini, F. & Holme, R., 2011. Reconstructing the Holocene geomagnetic field, *Earth planet. Sci. Lett.,* **312,** 497–505.

Kuang, W. & Bloxham, J., 1997. An Earth-like numerical dynamo model, *Nature,* **389,** 371–374.

Kuang, W. & Bloxham, J., 1999. Numerical modeling of magnetohydrodynamic convection in a rapidly rotating spherical shell: weak and strong field dynamo action, *J. Comp. Phys.,* **153,** 51–81.

Kuang, W., Tangborn, A., Jiang, W., Liu, D., Sun, Z., Bloxham, J. & Wei, Z., 2008. MoSST-DAS: The first generation geomagnetic data assimilation framework, *Comm. Comp. Phys.,* **3,** 85–108.

Kuang, W., Tangborn, A. & Wei, Z., 2009. Constraining a numerical geodynamo model with 100 years of surface observations, *Geophys. J. Int.,* **179,** 1458–1468.

Kuang, W., Wei, Z., Holme, R. & Tangborn, A., 2010. Prediction of geomagnetic field with data assimilation: a candidate secular variation model for IGRF-11, *Earth, Planets Space,* **62,** 775–785.

Langel, R.A. & Estes, R.H., 1982. A geomagnetic field spectrum, *Geophys. Res. Lett.,* **9,** 250–253.

Li, K., Jackson, A. & Livermore, P.W., 2011. Variational data assimilation for the initial-value dynamo problem, *Phys. Rev. E.,* **84,** doi:10.1103/PhysRevE.84.056321.

Licht, A., Hulot, G., Gallet, Y. & Thebault, E., 2013. Ensembles of low degree archeomagnetic field models for the past three millennia, *Phys. Earth planet. Inter.,* **224,** 38–67.

Liu, D., Tangborn, A. & Kuang, W., 2007. Observing system simulation experiments in geomagnetic data assimilation, *J. Geophys. Res.,* **112,** B08103, doi:10.1029/2006JB004691.

Lorenc, A., 1981. A global three-dimensional multivariate statistical interpolation scheme, *Mon. Wea. Rev.,* **109,** 701–721.

Lorenc, A., 1986. Analysis methods for numerical weather prediction, *Q.J.R. Meteorol. Soc.,* **112,** 1177–1194.

Nerger, L. & Hiller, W., 2013. Software for ensemble based data assimilation systems—implementation strategies and scalability, *Comput. Geosci.,* **55,** 110–118.

Richardson, L.F., 1922. *Weather Prediction by Numerical Process,* Cambridge Univ. Press.

Roberts, P.H., 1992. Geomagnetism, in *Encyclopedia of Earth System Science,* Vol. 2, pp. 277–294, ed. Nierenberg, W.A., Academic Press.

Sabaka, T.J., Olsen, N. & Purucker, M.E., 2004. Extending comprehensive models of the Earth's magnetic field with Ørsted and CHAMP data, *Geophys. J. Int.,* **159,** 521–547.

Sun, Z., Tangborn, A. & Kuang, W., 2007. Data assimilation in a Sparsly observed one-dimensional modeled MHD system, *Nonlin. Process. Geophys.,* **14,** 181–192.

Talagrand, O. & Courier, P., 1987. Variational assimilation of meteorological obserations with the adjoint vorticity equation, I: theory, *Q.J.R. Meteorol. Soc.,* **113,** 1311–1328.

Tangborn, A., Strow, L., Imbiriba, B., Ott, L. & Pawson, S., 2013. Evaluation of a new middle-lower tropospheric CO_2 product using data assimilation, *Atmos. Chem. Phys.,* **13,** 4487–4500.